Ferroelectricity from spin supercurrents in $LiCuVO_4$

M. Mourigal,[1,2] M. Enderle,[1] R. K. Kremer,[3] J. M. Law,[3] and B. Fåk[4]

[1]*Institut Laue-Langevin, BP156, 38042 Grenoble Cedex 9, France*
[2]*Laboratory for Quantum Magnetism, École Polytechnique Fédérale de Lausanne (EPFL), 1015 Lausanne, Switzerland*
[3]*Max-Planck Institute for Solid State Research, Heisenbergstrasse 1, 70569 Stuttgart, Germany*
[4]*Commissariat à l'Energie Atomique, INAC, SPSMS, 38054 Grenoble, France*

(Dated: March 22, 2011)

We have studied the magnetic structure of the ferroelectric frustrated spin-1/2 chain material $LiCuVO_4$ in applied electric and magnetic fields using polarized neutrons. A symmetry and mean-field analysis of the data rules out the presence of static Dzyaloshinskii-Moriya interaction, while exchange striction is shown to be negligible by our specific-heat measurements. The experimentally observed magnetoelectric coupling is in excellent agreement with the predictions of a purely electronic mechanism based on spin supercurrents.

PACS numbers: 77.80.-e, 75.10.Jm, 75.10.Pq, 71.70.Ej

Materials where ferroelectricity (FE) appears simultaneously with magnetic order are referred to as type-II or magnetic multiferroics. Considerable attention has been devoted to their unconventional magnetoelectric (ME) effects [1], namely the control of their electric polarization $\mathbf{P}$ with an external magnetic field $\mathbf{H}$ [2], and likewise at H=0 the favoring of a particular magnetic domain by an applied electric field $\mathbf{E}$ [3–7]. However, the fundamental mechanisms responsible for FE in this class of materials are under debate, in particular whether FE always results from atomic displacements or whether it can be induced by a purely electronic mechanism based on spin supercurrents [8] via the Aharonov-Casher effect, a relativistic topological quantum effect for neutral magnetic particles. Here, like in the spin Hall effect [9], the electric field directly controls the spin current without intermediating atomic displacements.

Phenomenologically, a spin spiral may induce an electric polarization $\mathbf{P} = A\,\mathbf{e}_{12}\times(\mathbf{S}_1\times\mathbf{S}_2)$, where $\mathbf{e}_{12}$ links neighboring spin sites $\mathbf{S}_1$ and $\mathbf{S}_2$ and A depends on the fundamental mechanism of the ME coupling [10]. Mechanisms that are experimentally established involve symmetry breaking lattice distortions, which are either induced by symmetric exchange [11] or by asymmetric Dzyaloshinskii-Moriya interaction (DMI) [12, 13]. The spin supercurrent mechanism [8], on the other hand, operates in the absence of magnetostriction and static DMI. Here frustration of the symmetric exchange interactions leads to non-collinear magnetic order and a spin supercurrent that couples to the electric field via the relativistic spin-orbit coupling (SOC). The sign and size of A is therefore materials specific [8, 14]. However, the spin supercurrent *vanishes* if the spin spiral is stabilized by DMI [8], and the latter is present in many materials, e.g. those studied in Refs. [4–7].

In this Rapid Communication, we provide strong experimental evidence that the ferroelectricity in the frustrated spin-1/2 chain material $LiCuVO_4$ is purely driven by the spin supercurrent mechanism [8, 14], and that magnetostriction is negligible. By combining mean-field theory and symmetry analysis with polarized neutron diffraction measurements of the magnetic structure in crossed electric and magnetic fields, we show that the static DMI plays no role in driving $LiCuVO_4$ to a spin-spiral ferroelectric state.

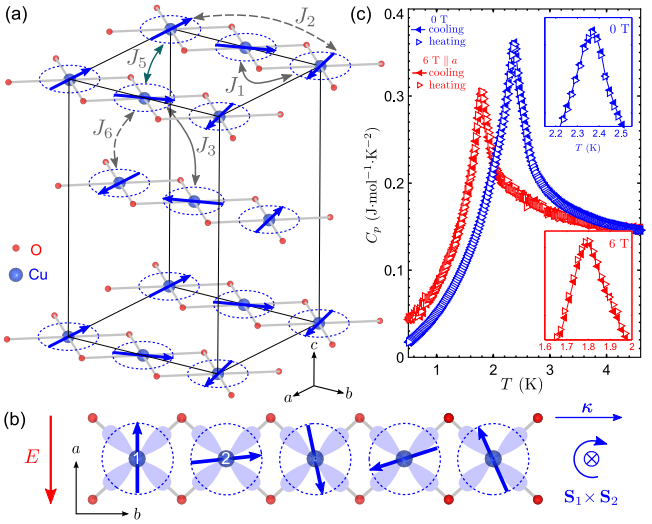

FIG. 1: (Color online) (a) Unit cell of $LiCuVO_4$ where only edge-sharing CuO_4 chains are shown. Solid (dashed) lines represent the ferromagnetic (antiferromagnetic) exchange interactions. (b) Isolated edge-sharing CuO_4 chain with single-hole $d_{x^2-y^2}$ orbitals and a $-im_b''$ cycloid. (c) Heat capacity at the magnetic transition shows absence of hysteresis between heating and cooling.

$LiCuVO_4$ crystallizes in the orthorhombic $Imma$ space group (#74), where the two Cu^{2+} ions in the primitive unit cell are located at the positions $\mathbf{r}_1 = (0,0,0)$ and $\mathbf{r}_2 = (0,1/2,0)$ [Fig. 1(a)]. They form spin–1/2 chains along the b axis built up from edge-sharing CuO_4 units. Below $T_N = 2.4$ K, three-dimensional antiferromagnetic (AFM) order sets in with an incommensurate propagation vector $\boldsymbol{\kappa} = (0,\kappa_y,0)$ with $\kappa_y = 0.532$ [15], stabilized

by frustration of nearest neighbor (J_1) ferromagnetic (FM) and next-nearest neighbor (J_2) AFM exchange interactions along the chain [16, 17]. Simultaneously, an electric polarization appears along the a axis [18]. In a magnetic field along the a axis, a spin-flop transition occurs at $H_a^{\rm SF}$=2.5 T [19, 20]. A concomitant flop of $\mathbf{P}$ from the a to the c axis is observed for $\mathbf{H} \parallel \boldsymbol{a}$, while no electric polarization is reported along b irrespective of the magnetic field direction above $H_b^{\rm SF}$ [21].

Heat-capacity measurements show that the magnetic order in $LiCuVO_4$ develops directly from the paramagnetic $Imma$ phase in a single second-order phase transition without any hysteresis within the accuracy (<5 mK) of the relaxation method of our Quantum Design calorimeter [Fig. 1(c)]. This indicates that symmetry breaking atomic displacements are negligible, which is also confirmed by our single-crystal neutron diffraction measurements below T_N.

We have determined the zero-field magnetic structure of $LiCuVO_4$ by reanalyzing the unpolarized neutron diffraction data of Ref. [15]. We find that the ordered Cu moments lie in the ab plane forming a planar spin spiral, which propagates along the b axis. This cycloid structure can be described in terms of Fourier components of the magnetic moments at the two Cu positions as $\mathbf{m}_1^{\boldsymbol{\kappa}} = (m_a, \pm i m_b'', 0)$ and $\mathbf{m}_2^{\boldsymbol{\kappa}} = -\mathbf{m}_1^{\boldsymbol{\kappa}} \exp(-i\pi\kappa_y)$ with m_a and m_b'' being real and positive. The $\pm$ sign corresponds to two possible chirality domains.

The population of these two chirality domains can be controlled by an electric field, as shown by our spherical neutron polarimetry measurements. In this technique, the directions of the incoming ($\mathbf{P}_i$) and outgoing ($\mathbf{P}_f$) neutron polarization can be chosen independently, using a so-called "cryopad" device [22]. This device was mounted on the thermal triple-axis spectrometer IN20 at the Institut Laue-Langevin. Polarized neutrons of wave vector 2.662 Å^{-1} were produced and analyzed by the (111) reflection of Heusler crystals as monochromator and analyzer, while second-order (unpolarized) neutrons were removed by a PG(002) filter in the scattered beam. A single crystal of $LiCuVO_4$ of size 1.9 × 0.7 × 5 mm^3 was aligned in the bc plane and cooled down to T=1.5 K in a vertical electric field $E_a \simeq 45$ kV/m pointing in the $-\boldsymbol{a}$ direction. Scans along $(0k0)$ were performed for magnetic Bragg reflections $(0, \pm\kappa', \pm\ell)$ with $\ell = 1, 3, 5$, and $\kappa' = 1 - \kappa_y = 0.47$. Introducing a cartesian coordinate system with $\hat{\mathbf{x}}$ along $\mathbf{Q}$, $\hat{\mathbf{y}}$ perpendicular to $\mathbf{Q}$ in the scattering plane, and $\hat{\mathbf{z}}$ perpendicular to the scattering plane, the neutron cross-section for $\mathbf{P}_i$ along $\hat{\mathbf{y}}$ and $\mathbf{P}_f$ along $\pm\hat{\mathbf{x}}$ is $\sigma_{yx,y\bar{x}} \propto \frac{1}{2}(|\mathbf{M}_{\perp\mathbf{Q}}|^2 \mp i[\mathbf{M}_{\perp\mathbf{Q}}^* \times \mathbf{M}_{\perp\mathbf{Q}}]\cdot\hat{\mathbf{x}})$. Here, $\mathbf{M}_{\perp\mathbf{Q}} = \mathbf{Q} \times [\mathbf{M}(\mathbf{Q}) \times \mathbf{Q}]/|\mathbf{Q}|^2$ is the component of the magnetic structure factor, $\mathbf{M}(\mathbf{Q}) = \sum_j \mathbf{m}_j^{\boldsymbol{\kappa}} \exp(i\mathbf{Q}\cdot\mathbf{r}_j)$, that is perpendicular to the wave-vector transfer $\mathbf{Q} = (h, k, \ell)$. We note that the chiral term $i[\mathbf{M}_{\perp\mathbf{Q}}^* \times \mathbf{M}_{\perp\mathbf{Q}}]$ is either parallel or anti-parallel to $\mathbf{Q}$.

Figure 2(a) shows the resulting $\sigma_{yx,y\bar{x}}$ cross-sections for

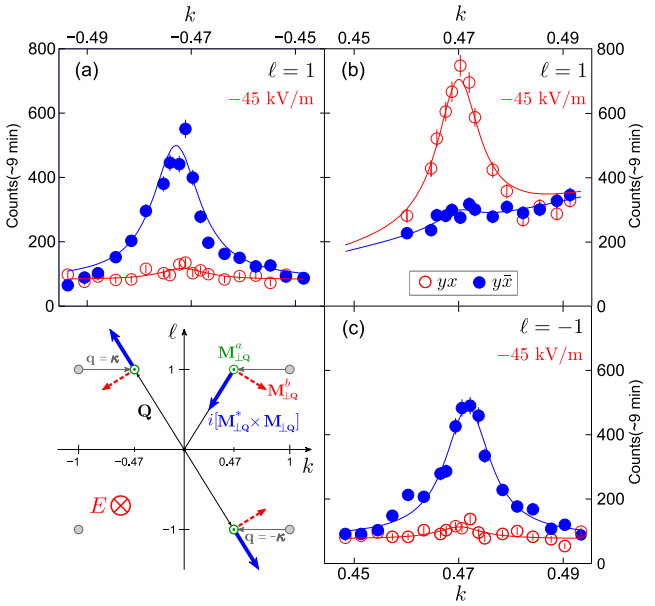

FIG. 2: (Color online) (a–c) Neutron polarization dependence of the magnetic reflections $(0, \pm 0.47, \pm 1)$ at T=1.5 K with an electric field E_a directed along the $-\boldsymbol{a}$ direction. The lower-left panel is a sketch of the Brillouin zone in the bc plane.

the magnetic Bragg peak $(0, -\kappa', 1)$. For the cycloid with $-im_b''$ sketched in Fig. 1(b), the b component of $\mathbf{M}(\mathbf{Q})$ is negative (the dashed red arrow shows its projection $\perp \mathbf{Q}$), which implies that the chiral term $i[\mathbf{M}_{\perp\mathbf{Q}}^* \times \mathbf{M}_{\perp\mathbf{Q}}]$ in the cross-section is parallel to $\mathbf{Q}$. Intensity should then be observed only in the $\sigma_{y\bar{x}}$ channel, which is the case. At $\mathbf{Q} = (0, \kappa', 1)$ [Fig. 2(b)], the direction of the propagation vector $\boldsymbol{\kappa}$ is reversed, which in turn reverses the b component of $\mathbf{M}(\mathbf{Q})$, since $\mathbf{m}_j^{-\boldsymbol{\kappa}} = (\mathbf{m}_j^{\boldsymbol{\kappa}})^*$. The sign of the chiral term is therefore reversed, i.e. it is anti-parallel to $\mathbf{Q}$, and intensity is observed in σ_{yx}, still corresponding to the same chirality of the cycloid ($-im_b''$). At $\mathbf{Q} = (0, \kappa', -1)$ [Fig. 2(c)], the directions of both $\mathbf{Q}$ and $\boldsymbol{\kappa}$ are reversed, and the situation of Fig. 2(a) is recovered. Cooling the sample in zero electric field leads to equal intensity in the two polarization channels, which implies that both domains are equally populated. From these observations we conclude that an electric field $\mathbf{E} \parallel \boldsymbol{a}$ controls the chiral domain population and that the ME coupling is negative, $A < 0$, since the populated domain has $\mathbf{e}_{12} \times (\mathbf{S}_1 \times \mathbf{S}_2)$ anti-parallel to $\mathbf{P}$ (and $\mathbf{E}$).

To obtain more quantitative information on the magnetic structure for $\mathbf{E} \parallel \boldsymbol{a}$, we modeled all 36 polarized cross sections $\sigma_{\alpha\beta}$ $(\alpha, \beta = \pm x, \pm y, \pm z)$ of the five magnetic Bragg peaks measured using a more general $\mathbf{m}_1^{\boldsymbol{\kappa}} = (m_a, m_b' + i m_b'', 0)$, i.e. allowing m_b to have a real component in addition to the imaginary one considered until now. A least-squares fit was performed with m_a, m_b', m_b'', and d_- as free parameters, where d_- is the domain population of the $-im_b''$ domain. The resulting parameters $m_b' = 0.01(5)\, m_a$, $m_b'' = 0.95(3)\, m_a$, and

d_-=0.99(2) establish that the zero-field magnetic structure is a *circular* cycloid in the *ab* plane with a single chirality domain fully populated. A similar fit of two reflections measured with E=0 gave an equal domain population, i.e. d_-=d_+=0.50(0), which strongly supports the conclusion that full control of the cycloid chirality is achieved by applying an electric field along *a*.

These results are confirmed when a magnetic field **H** is applied close to the *c* axis, in which case no spin-flop transition is expected nor observed. In order to detect the chiral term we used the same *bc*-oriented sample as before with a magnetic field in the horizontal scattering plane and a vertical electric field $\mathbf{E} \parallel \boldsymbol{a}$. Compared to the previously described set-up, we used an unpolarized incoming beam from a Si(111) monochromator but kept polarization analysis and a spin flipper in the scattered beam. In this configuration, $\mathbf{P}_f$ is parallel or anti-parallel to **H**. The neutron polarization for a sample cooled in a positive electric field is shown in Fig. 3(b), and, following the same reasoning as for Fig. 2, corresponds to a cycloid with $+im_b''$. The sample was then warmed up to 10 K, well above T_N, and cooled down in a reversed electric field. This leads to a complete inversion of the chiral domain population [Fig. 3(c)]. Complementary measurements with H=3.5 T exactly along the *c* axis corroborate these findings [see Fig. 3(d)]. From this, we conclude that the *ab* cycloid is stable upon application of $\mathbf{H} \parallel \boldsymbol{c}$ up to at least 3.5 T and that an electric field along $\pm\boldsymbol{a}$ fully controls the chirality of the cycloid. Furthermore, we find that the ME coupling is negative, $A<0$, as in zero magnetic field.

A crucial test of the validity of the spin supercurrent model for $LiCuVO_4$ is to raise the magnetic field above the spin-flop field $H_a^{\rm SF}$, where theory predicts a cycloid in the *bc* plane, which according to Ref. [14] results in a positive ME coupling, $A>0$. Measurements were performed on a 4.5 × 3.5 × 1 mm^3 single crystal aligned in the *ab* plane and cooled down with $\mathbf{H} \parallel \boldsymbol{a}$=3.8 T and $\mathbf{E} \parallel +\boldsymbol{c}$ as sketched in Fig. 3(e). A magnetic peak was found at $\mathbf{Q}$=$(1,\kappa',0)$, which confirms the stability of the propagation vector $\boldsymbol{\kappa}$ for $H_a > H_a^{\rm SF}$. As shown in Fig. 3(f–h), $\mathbf{P}_f$ changes sign when **E** is reversed (under field-cooled conditions) and essentially vanishes for zero electric field. For an electric field $\mathbf{E} \parallel +\mathbf{c}$ $(-\mathbf{c})$ of 150 (130) kV/m, we observe a circular cycloid given by $\mathbf{m}_1^{\boldsymbol{\kappa}} = (0, m, \pm im)$ with $+im$ $(-im)$ and a domain population of d_+=0.87 (d_-=0.78) [Fig. 3(f–g)], while for zero electric field an equal domain population is observed, d_+=0.55(2) [Fig. 3(h)]. We conclude that an electric field along the *c* axis controls the magnetic domain population of the spin cycloid observed above the spin-flop field, at H_a= 3.8 T. The chirality of the cycloid is such that the ME coupling constant A is positive for the *bc*-plane structure, $A>0$.

Symmetry analysis, which is directly applicable since there is only one second order phase transition, leads

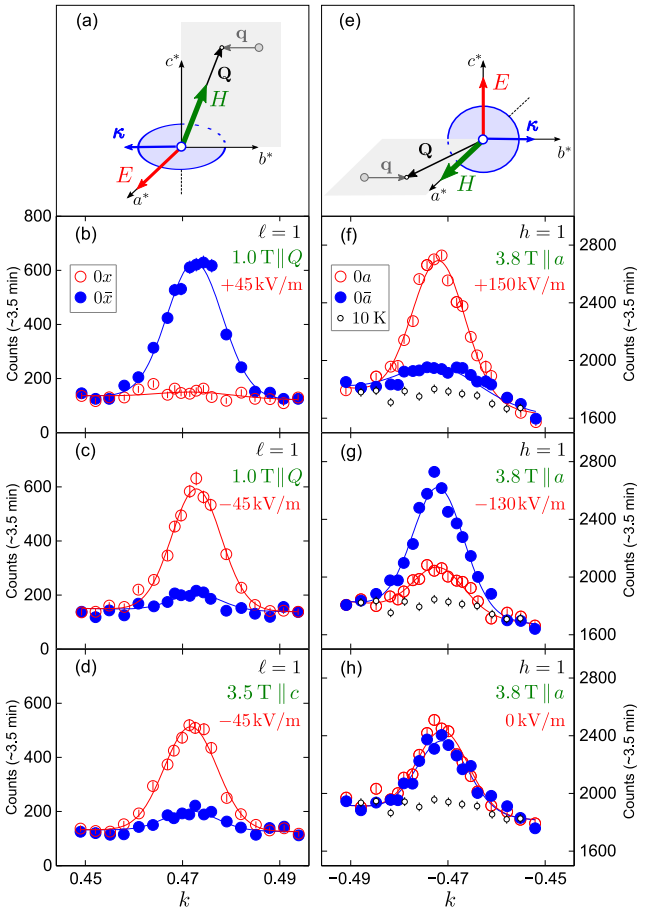

FIG. 3: (Color online) (a–d) Neutron polarization dependence of the magnetic reflection $(0, 0.47, 1)$ at T=2.1 K with $E_a \simeq \pm 45$ kV/m and H=1 T along **Q** as sketched in (a) or H=3.5 T along **c**. (e–g) Similar scans for $(1, -0.47, 0)$ at T=1.9 K with $E_c \neq 0$ and H_a =3.8 T along $\boldsymbol{a}$ as sketched in (e). The E_c<0 value had to be reduced with respect to E_c>0 due to electric discharges. (h) Same scans for E=0. Identical results are obtained with the direction of **H** reversed.

to four one-dimensional irreducible representations (IR), none of which can describe the observed *ab* cycloid. To proceed, we calculate the mean-field ground-state energy, $\varepsilon_{\rm gs}(\boldsymbol{\kappa}) = \sum_{\boldsymbol{\kappa}} \sum_{ij} [\mathbf{S}_i(-\boldsymbol{\kappa}) \mathbf{J}_{ij}(\boldsymbol{\kappa}) \mathbf{S}_j(\boldsymbol{\kappa})]$, where $\mathbf{J}_{ij}(\boldsymbol{\kappa})$ is a (complex) 6 × 6 matrix representing the Fourier-transformed exchange interactions. Imposing the symmetry constraints of the *Imma* space group on $\mathbf{J}_{ij}(\boldsymbol{\kappa})$ leads to cancelation of all off-diagonal terms except terms of type *yz*. This implies that the DMI term of type *xy* (D_z) is zero for *every* bilinear exchange path, which precludes the stabilization of an *ab* cycloid by DMI. A *bc*-cycloid cannot be stabilized either by DMI, since the *yz* (D_x) term alternates in sign along the chain. If we impose as constraints our experimental findings that h+l is odd, m_c=0, and that the magnetic structure contains both m_a and m_b components, it follows from minimizing $\varepsilon_{\rm gs}(\boldsymbol{\kappa})$ that the exchange matrix is pseudo-

tetragonal for all dominant exchange paths defined in Ref. [16], unless there are pathological coincidences of the exchanges. The cycloid is then stabilized in the *ab* plane by a diagonal exchange anisotropy of easy-plane type, $|J_z| < |J_x| = |J_y|$. Imposing as maximum spin value $S{=}\frac{1}{2}$ on both Cu sites, we find that the general Fourier component of site 1, $\mathbf{m}_1^{\boldsymbol{\kappa}} = (m_a, \pm[m'_b + im''_b], 0)$, is reduced to $\mathbf{m}_1^{\boldsymbol{\kappa}} = (m, \pm im, 0)$ with m real. This corresponds to the combination of two irreducible representations with equal amplitude in quadrature and represents two degenerate perfectly circular cycloids of either rotation sense, in agreement with our experimental findings. From these mean-field considerations, we conclude that the zero-field spin-cycloid of $LiCuVO_4$ occurs without stabilizing DMI, driven exclusively by frustrated anisotropic diagonal (pseudo-tetragonal) exchange.

A magnetic field applied in the *ab* plane leads to a spin-flopped cycloid or helix in a plane perpendicular to the field as soon as the Zeeman energy overcomes the anisotropic diagonal exchange. Our finding of a (near) single-domain spin-flopped *bc*-plane cycloid for $H_a > H_a^{\mathrm{SF}}$ and $\mathbf{E} \parallel \boldsymbol{c}$ with the same propagation vector as before and a chirality that depends on the sign of the electric field confirms the purely diagonal exchange scheme, and is quite distinct from the complex behavior of other materials [13]. The anisotropy of the diagonal exchange energy calculated within mean-field theory using the spin-flop field of 2.5 T and the main exchange integrals from Ref. [16] is less than $\sim$0.5%. Similar energy considerations for the spin-flop field put an upper limit on the ratio of off-diagonal (yz) and diagonal exchange energy to less than $4{\cdot}10^{-4}$. The exchange matrix of $LiCuVO_4$ is hence remarkably isotropic, with diagonal anisotropic exchange being the leading (small) perturbation. This pseudo-tetragonal spin symmetry of the exchange matrix has its origin in the almost tetragonal symmetry of the CuO_6 octahedron and the perfectly flat edge-shared CuO_4 chains in the *ab* plane of $LiCuVO_4$. The latter lead to a pseudo-tetragonal exchange matrix even in the presence of a small (orthorhombic) distortion of the bond angles away from 90° [23].

By combining our experimental results with mean-field calculations, we have shown that the formation of a ferroelectric spin-cycloid in $LiCuVO_4$ below T_N is driven by purely diagonal frustrated anisotropic exchange without stabilizing static DMI or magnetostriction. This rules out most of the currently discussed mechanisms for FE except the spin supercurrent scenario [8]. This purely electronic scenario has been studied for both linear Cu–O–Cu clusters of e_g electrons [24] and for edge-sharing CuO_4 geometry [14, 23, 25]. In the latter case, SOC has been shown to generate a small symmetric exchange anisotropy [23] as well as Coulombic ring-exchange processes [23, 25], which lead to chiral correlations and finally ME coupling [25]. Tetramer diagonalization and first-principles calculations of the SOC on O- and Cu-sites of $LiCuVO_4$ show that the spin supercurrent creates FE polarization in the absence of atomic displacements, only by asymmetric orbital occupancy [14]. These calculations predict the sign change of the ME constant A at the spin-flop transition for $\mathbf{H} \parallel \boldsymbol{a}$ that we observe experimentally.

We conclude that the purely electronic scenario of spin supercurrents is realized in $LiCuVO_4$: a small symmetric exchange anisotropy is present while magnetostriction and static DMI are negligible, and the theoretical predictions of both the ratio of the electric polarizations P_a/P_c and the sign of the ME coupling in all ferroelectric phases are found in excellent agreement with experiments.

We acknowledge fruitful discussions with J. Schweizer, G. Nenert, T. Ziman, and M. E. Zhitomirsky and experimental assistance from P. Steffens, P. Chevalier, E. Bourgeat-Lami (neutrons), and G. Siegle (specific heat).

[1] S.W. Cheong and M. Mostovoy, Nat. Mat. **6**, 13 (2007); Y. Tokura and S. Seki, Adv. Mater. **22**, 1554 (2010).
[2] T. Kimura *et al.*, Nature (London) **426**, 55 (2003); M. Kenzelmann *et al.*, Phys. Rev. Lett. **95**, 087206 (2005); N. Aliouane *et al.*, Phys. Rev. Lett. **102**, 207205 (2009).
[3] P.G. Radaelli *et al.*, Phys. Rev. Lett. **101**, 067205 (2008).
[4] Y. Yamasaki *et al.*, Phys. Rev. Lett. **98**, 147204 (2007).
[5] S. Seki *et al.*, Phys. Rev. Lett. **100**, 127201 (2008).
[6] I. Cabrera *et al.*, Phys. Rev. Lett. **103**, 087201 (2009).
[7] T. Finger *et al.*, Phys. Rev. B. **81**, 054430 (2010).
[8] H. Katsura, N. Nagaosa, and A. V. Balatsky, Phys. Rev. Lett. **95**, 057205 (2005).
[9] S. Murakami, N. Nagaosa, and S.C. Zhang, Science **301**, 1348 (2003).
[10] M. Mostovoy, Phys. Rev. Lett. **96**, 067601 (2006).
[11] P.G. Radaelli *et al.*, Phys. Rev. B **79**, 020404(R) (2009).
[12] I. A. Sergienko and E. Dagotto, Phys. Rev. B **73**, 094434 (2006).
[13] M. Mochizuki and N. Furukawa, Phys. Rev. Lett. **105**, 187601 (2010).
[14] H. J. Xiang and M.-H. Whangbo, Phys. Rev. Lett. **99**, 257203 (2007). The sign of **P** is clarified in Refs. 9,28 of H. J. Xiang *et al.*, Phys. Rev. Lett. **101**, 037209 (2008).
[15] B. J. Gibson *et al.*, Physica B **350**, 253(E) (2004).
[16] M. Enderle *et al.*, Europhys. Lett. **70**, 237 (2005).
[17] M. Enderle *et al.*, Phys. Rev. Lett. **104**, 237207 (2010).
[18] Y. Naito *et al.*, J. Phys. Soc. Jpn. **76**, 023708 (2007); Y. Yasui *et al.*, J. Phys. Soc. Jpn. **77**, 023712 (2008).
[19] M. G. Banks *et al.*, J. Phys.: Condens. Matter **19**, 145227 (2007).
[20] N. Büttgen *et al.*, Phys. Rev. B. **76**, 014440 (2007).
[21] F. Schrettle *et al.*, Phys. Rev. B. **77**, 144101 (2008).
[22] P. J. Brown *et al.*, Proc. R. Soc. A **442**, 147 (1993).
[23] S. Tornow, O. Entin-Wohlman, and A. Aharony, Phys. Rev. B. **60**, 10206 (1999).
[24] C. Jia, S. Onoda, N. Nagaosa, and J. H. Han, Phys. Rev. B **76**, 144424 (2007).
[25] S. Onoda and N. Nagaosa, Phys. Rev. Lett. **99**, 027206 (2007).